ARTICLE NO. 80-4132

Wall Temperatures and Solar Deflection of Cylindrical Structures in Space

Masao Furukawa*
National Space Development Agency of Japan, Tokyo, Japan

Analytical expressions are presented which describe wall temperatures for a quasisteady state in a long, thin-walled cylinder subjected to periodic solar heating. Another expression is also presented which gives a steady-state circumferential temperature distribution of a discontinuous cylindrical tube with a locked overlapped cross section. Such a cylinder or tube is considered to represent a gravity gradient rod of seam or seamless fabrication. A relatively long space telescope is also regarded as such a cylinder. The analysis takes into account internal radiation exchange which has been neglected thus far because of its complexity. Two different sorts of solution methods associated with Laplace transformation are developed for obtaining closed-form solutions of governing integrodifferential equations: the Fourier series expansion technique and the Ritz procedure related to the variational principle. Parametric studies are made to evaluate the effects of surface properties, multilayer insulation, and circumferential heat pipes upon the temperature uniformity and constancy of large space telescopes. For a rod of the overlap type, the variational method is employed as an analytical means which can deal with the overlapped portion. By making the zero twist assumption, thermal bending moments about the principal axes are derived from direct integration of the circumferential temperature distribution. Numerical computations are performed to verify the analytical results and to predict the thermal behavior of a typical gravity gradient rod. The effect of radiant interchange upon the solar deflection is discussed with a specific example in which internal radiation is negligible.

Nomenclature

A = Fourier coefficient defined in Eq. (36)
a = coefficient defined in Eqs. (41), (46), (70a), (B3), or (B5)
B = differential absorption factor, given in Eqs. (A1) or (C1)
b = coefficient defined in Eqs. (70b), (B4), or (B6)
C = specific heat
c = coefficient defined in Eqs. (60) or (70c)
e_T = thermal coefficient of expansion
f = coefficient defined in Eqs. (A5) or (D1)
f_s = solar heat input function, given in Eqs. (4) or (63)
G = Young's modulus of elasticity
g = coefficient defined in Eq. (B1)
h = wall thickness
I = area moment of inertia, given in Eqs. (80) or (86)
I_s = solar constant
i = dimensionless moment of inertia, given in Eq. (81)
J = functional defined in Eqs. (17), (58), or (66)
K = coefficient defined in Eq. (D6)
k = radiation conductance
k_0 = effective radiation conductance, defined in the first expression of Eq. (27)
L = tube length
l = dimensionless length, defined in the second expression of Eq. (1)
M = thermal bending moment, given in Eqs. (76) or (85)
m = dimensionless thermal bending moment, given in Eq. (77)
N_0 = number of sheets of multilayer insulation
P = periodic unit step function, defined in Eq. (11)
p = coefficient defined in Eq. (23)
q_0 = absorbed solar energy, given in Eq. (3)
R = exponential-like step function, defined in Eq. (26)
r = tube radius
s = Laplace parameter
T = absolute temperature
$\bar{T}$ = reference temperature, defined in Eqs. (8) or (50)
T_B = mean temperature of space telescope associated with heat pipes, defined in Eq. (53)
t = time
t_0 = orbital period
u = emissive power, defined in Eq. (5)
v = Laplace transform of u, defined in Eq. (12)
W = half interval of heat pipes spaced at regular intervals
w = expression defined in Eq. (20)
x,y = position coordinates on circumference measured from the center of mass, given in Eqs. (75) or (84)
Z = axial length coordinate
z = dimensionless coordinate, defined in the first expression of Eq. (1) or in Eq. (47)
α = solar absorptance
β = coefficient defined in the first or second expressions of Eq. (10)
γ = coefficient defined in the third expression of Eq. (10)
γ' = coefficient defined in Eq. (57)
ΔL = thermal contraction, given in Eq. (32)
δ = boom tip deflection, given in Eqs. (82) or (87)
ϵ = infrared emittance
ζ = sunlit factor ($1-\zeta$ = eclipse factor)
η = unit step function
θ = dimensionless temperature, defined in Eq. (54)
θ_s = solar elevation angle, shown in Fig. 1
λ = heat conductivity
λ_0 = constant defined in the second expression of Eq. (27)
μ = factor defined in Eqs. (A2) or (C2)
ξ = dimensionless variable
ρ = density
ρ_D = diffuse component of reflectance
ρ_S = specular component of reflectance
σ = Stefan-Boltzmann constant
σ_z = thermal stress, given in Eq. (73)
τ = dimensionless time, defined in Eq. (6)
τ_S = rate of surface nondiffusiveness = $\rho_S/(\rho_S+\rho_D)$
ϕ = overlap angle, shown in Fig. 1
ϕ' = total perimeter of cross section, defined in Eq. (61)

Received July 30, 1979; revision received March 14, 1980.

Index category: Radiation and Radiative Heat Transfer.
*Engineer, First Group of Satellite Design.

φ = angular position on circumference
φ_s = solar azimuth angle, shown in Fig. 1
ψ = angular variable
Ω = out-of-sunline angle, defined in Eq. (83), or solution of Eq. (24)
ω = solution of Eqs. (28) or (38), or constant defined in Eq. (43)

Subscripts

0 = multilayer insulation
s = sun
x,y = x and y component, respectively
∞ = thermal equilibrium state
max = maximum in quasisteady state
min = minimum in quasisteady state

Introduction

TUBULAR extendible elements or storable extendible members have been put to use as gravity gradient rods in attitude stabilization and as extremely long antennas in electric field measurement. They are usually thin, metallic ribbons rolled into tubes along their longitudinal axis, and commonly referred to as booms. When a boom is deployed, it takes the form of a simply overlapped, cylindrically shaped tube of long length. Because of its long, slender structure, thermal bending induced by solar heating may cause large tip deflections which will seriously affect the boom pointing accuracy and the gravity gradient system stability. It is, therefore, essential to make an estimate of temperature gradients responsible for thermal bending.

Frisch[1] investigated the static thermal equilibrium shape of a boom bent and twisted by thermal stresses in order to incorporate it into a dynamic model of gravity-gradient-type satellites. Florio and Hobbs[2] gave an analytical expression of circumferential temperature distributions in a rod of the overlap type, and presented some test results demonstrating the validity of their method of solution. Eby and Karam[3] derived a single expression which seems more convenient than this[2] to estimate the circumferential temperature distribution. They also studied the thermal bending for various combinations of overlap angles and solar directions, and found the optimal overlap angle which minimizes the maximum possible deflection.

Although the conventional analyses[1-3] have been successfully employed for engineering design, there exists a limit in applicability. This is due to the assumption that the effect of internal radiation exchange can be neglected. However, in some recent booms, the radiant interchange is not as small as thought earlier. Thus this effect must be accounted for in the advanced analysis. Fixler[4] solved the thermal balance equation numerically by including an integral term expressing interradition. But his method is applicable only to booms of seamless fabrication. After that, Graham[5] analyzed the radiative transfer in a long cylinder with a gray, diffuse surface. Further development of their analyses[1-5] is necessary to obtain analytical results applicable to every type of boom.

Large space telescopes were designed to meet the needs of astronomers, but some thermal problems remain to be solved prior to attaining their mission. Thermal control is regarded as the most critical item in their design and construction because of the mandatory requirement that the thermal distortions incurred along the tube axis be extremely small.[6] Studies relating to thermal control of large space telescopes were carried out in detail by Katzoff.[7,8] He presented many numerical examples showing the degree of temperature uniformity attainable by various means involving application of isothermalizer heat pipes. However, his method is inapplicable to estimation of the temperature variation caused by the alternating sunlight and shadow phases in a low-altitude orbit, in spite of the fact that an eclipse is the chief factor in thermal distortions. This restriction and some unreasonable assumptions, such as no heat conduction and a black wall surface, impose a considerably large limit on the applicability of his analytical approach. A generalization of his analysis is therefore desirable.

The present study is performed in such a way that a unified treatment is possible for the thermal problems related to large space telescopes and booms of seam or seamless fabrication. For mathematical formulations of the radiation heat transfer around the interior of a cylinder, this paper employs the absorption factor method developed by Gebhart.[9] The use of the absorption factor brings forth nonlinear integrodifferential equations governing the heat transfer. Analytical solutions of the linearized equation are presented which allow direct computation of wall temperature distributions on a cylinder wrapped in multilayer insulation and exposed to periodic solar heating. They can be used for evaluation of the temperature uniformity and constancy of a large space telescope. In the case of no insulation, the solution reduces to the expression of wall temperatures of a boom of seamless fabrication. Application of circumferential heat pipes to a relatively long space telescope is also analyzed to investigate their effect on circumferential temperature uniformity. For a commonly used boom with an overlapped cross section, an approximate solution based upon the variational method is presented for estimating the amount of tip deflections and out-of-sunline angles. Numerical computations are made for a typical boom to demonstrate the applicability of the analytical results.

Response to Periodic Solar Heating

General Formulation

One first considers an insulated cylinder, being r in radius and L in length, with a perfect flat mirror at its closed end ($Z=0$). Then one employs the coordinate system in which the central axis is taken as the Z axis. For simplicity, all length quantities are hereafter placed in the following dimensionless forms:

$$z=Z/r \qquad l=L/r \tag{1}$$

Since the mirror reflects the interior, this configuration is identical with a cylinder of unit radius and $2l$ length with both ends open ($z=\pm l$). Although the secondary mirror, the hole at the center of the primary mirror, the instrument structure, etc., are not taken into account, such a cylinder provides a simple, idealized model that should serve as a first approximation to any eventual design of a large space telescope.

Because of the thin wall thickness, the radial temperature gradient can be neglected in the wall. Thus the wall temperature will be considered as a function of the longitudinal distance z and the angle φ from the subsolar point. The solar energy is absorbed in the outside surface of the multilayer insulation in which the telescope is wrapped. A part of this absorbed energy is released to space by radiation, while the remaining part is transferred through the insulation. According to some experimental results,[7] the heat flow through the insulation is proportional to the emissive power difference between the outermost sheet and the cylinder wall. This heat supply is characterized by radiation conductance, the concept of which was introduced by Katzoff[7] in order to account for the effect of a number of sheets, and distributed over the interior by both conduction and internal radiation exchange. It is then assumed that the temperature is uniform over the outermost sheet of the insulation.

Mathematical formulations of the above heat-transfer phenomena lead to the following integrodifferential equations for the telescope with constant thermal properties:

$$C_0\rho_0N_0\frac{dT_0}{dt}=q_0f_s(\varphi)P(t;t_0\zeta)-\epsilon_0\sigma T_0^4-k(\sigma T_0^4-\sigma T^4) \tag{2a}$$

$$C\rho h\frac{\partial T}{\partial t}=\frac{\lambda h}{r^2}\left(\frac{\partial^2 T}{\partial\varphi^2}+\frac{\partial^2 T}{\partial z^2}\right)-k(\sigma T^4-\sigma T_0^4)-\epsilon\sigma T^4$$

$$+\epsilon\int_{-l}^{l}\int_{0}^{2\pi}\sigma T^4(\xi,\psi)B(\xi,\psi;z,\varphi)\,\mathrm{d}\xi\mathrm{d}\psi \qquad (2b)$$

where q_0 is expressed as follows in considering the solar direction:

$$q_0=\alpha_0 I_s\sin\theta_s \qquad (3)$$

In Eqs. (2), no heat source other than the solar radiation is taken into account. Solar heat input is neglected in Eq. (2b) because of the sun shield attached to the aperture of the telescope. Since one-half of the outside surface receives no radiation at all, the solar heat input function $f_s(\varphi)$ is written as

$$f_s(\varphi)=\begin{cases}\cos\varphi & \text{if } 0\le\varphi<\pi/2 \text{ or } 3\pi/2<\varphi\le 2\pi\\ 0 & \text{if } \pi/2\le\varphi\le 3\pi/2\end{cases} \qquad (4)$$

The presence of an eclipse in the orbit is represented in terms of a periodic unit step function $P(t;t_0\zeta)$ which is equal to one in sunlit phases and to zero in shadow phases. Also the inner surface is assumed to be a gray, diffuse emitter which allows both diffuse and specular reflections in accordance with the relation $\epsilon+\rho_S+\rho_D=1$. The kernel $B(\xi,\psi;z,\varphi)$ in the integral term of Eq. (2b) is the differential absorption factor between two infinitesimal area elements, $\mathrm{d}A$ and $\mathrm{d}A'$, which are located at $(\cos\varphi, \sin\varphi, z)$ and $(\cos\psi, \sin\psi, \xi)$, respectively. This factor shows the proportion of radiation emitted from $\mathrm{d}A$ which is eventually absorbed at $\mathrm{d}A'$.

As the basic variables, one takes now the emissive power and the dimensionless time:

$$u=\sigma T^4 \qquad u_0=T_0^4 \qquad (5)$$

$$\tau=t/t_0 \qquad (6)$$

In addition to this change, the following approximations proposed by Katzoff[7] are employed in order to transform Eqs. (2) into a simpler form:

$$\frac{\partial T}{\partial t}\approx\frac{1}{4\sigma\bar{T}^3 t_0}\frac{\partial u}{\partial\tau},\ \frac{\partial^2 T}{\partial\varphi^2}\approx\frac{1}{4\sigma\bar{T}^3}\frac{\partial^2 u}{\partial\varphi^2},\ \frac{\partial^2 T}{\partial z^2}\approx\frac{1}{4\sigma\bar{T}^3}\frac{\partial^2 u}{\partial z^2} \qquad (7)$$

The error introduced by Eq. (7) may be reduced by defining $\bar{T}$ as the temperature satisfying the following relation:

$$\bar{T}=(q_0\zeta/\pi\epsilon_0\sigma)^{1/4} \qquad (8)$$

Equation (8) shows that the integrated absorbed solar flux is equal to the heat radiated at $\bar{T}$. Rewriting Eqs. (2) by using Eqs. (5-7), one has the following integrodifferential equation which is soluble by analytical means:

$$\beta_0\frac{\mathrm{d}u_0}{\mathrm{d}\tau}=q_0 f_s(\varphi)P(\tau;\zeta)-\epsilon_0 u_0-k(u_0-u)$$

$$\beta\frac{\partial u}{\partial\tau}=\gamma\left(\frac{\partial^2 u}{\partial\varphi^2}+\frac{\partial^2 u}{\partial z^2}\right)-k(u-u_0)-\epsilon u$$

$$+\epsilon\int_{-l}^{l}\int_{0}^{2\pi}u(\xi,\psi)B(\xi,\psi;z,\varphi)\,\mathrm{d}\xi\mathrm{d}\psi \qquad (9)$$

where β_0, β, and γ are defined as

$$\beta_0=\frac{C_0\rho_0 N_0}{4\sigma\bar{T}^3 t_0} \qquad \beta=\frac{C\rho h}{4\sigma\bar{T}^3 t_0} \qquad \gamma=\frac{\lambda h}{4\sigma\bar{T}^3 r^2} \qquad (10)$$

The function $P(\tau;\zeta)$ is expressible in the following superposition of unit step functions, because it simply shows a dimensionless form of $P(t;t_0\zeta)$:

$$P(\tau;\zeta)=\sum_{m=0}^{\infty}\{\eta(\tau-m)-\eta(\tau-m-\zeta)\} \qquad (11)$$

Although the form of Eq. (11) seems rather complicated, its Laplace image with respect to τ has a relatively simple form. For this reason, the analysis is facilitated by means of a Laplace transformation. The variables u and u_0 are now replaced by their image functions v and v_0:

$$v(s)=\mathcal{L}\{u(\tau)\}=\int_0^\infty u(\tau)e^{-s\tau}\mathrm{d}\tau,\quad v_0(s)=\mathcal{L}\{u_0(\tau)\} \qquad (12)$$

Thus Eqs. (9) are transformed into integral equations of v and v_0 from which v_0 is eliminated. Omitting the initial values $u(0)$ and $u_0(0)$ which are not important, one has the following final equation to solve:

$$\left\{\beta s+\epsilon+\frac{k(\beta_0 s+\epsilon_0)}{\beta_0 s+\epsilon_0+k}\right\}v$$

$$=\gamma\left(\frac{\partial^2 v}{\partial\varphi^2}+\frac{\partial^2 v}{\partial z^2}\right)+\frac{kq_0}{s(\beta_0 s+\epsilon_0+k)}\frac{1-e^{-s\zeta}}{1-e^{-s}}f_s(\varphi)$$

$$+\epsilon\int_{-l}^{l}\int_{0}^{2\pi}v(\xi,\psi)B(\xi,\psi;z,\varphi)\,\mathrm{d}\xi\mathrm{d}\psi \qquad (13)$$

Now attention can be turned to the state of particular interest, that is, the quasisteady state in which the same temperature variation is repeated every revolution as a result of periodic heating. Such an idealized state will exist after many revolutions in orbit. As easily seen from the form of the heat input function given by Eq. (11), the temperature reaches a maximum at the end of each sunlit phase and a minimum at the beginning. The maximum and minimum temperature distributions are, therefore, derived from the Laplace transform inversion of the solution of Eq. (13) in the following fashion:

$$u_{\max}=\lim_{m\to\infty}u(m+\zeta) \qquad u_{\min}=\lim_{m\to\infty}u(m) \qquad (14)$$

Then the equilibrium temperature distribution is readily found by putting $\zeta=1$ in Eq. (14), because the thermal equilibrium state can be regarded as a special case of quasisteady states.

Axial Temperature Distribution

If circumferential temperature gradients are negligibly small, the problem is then greatly simplified. Such a case is practically realized by applying circumferential heat pipes. In this case, the temperature depends on z only. Equation (13) thereby reduces to the following expression:

$$\left\{\beta s+\epsilon+\frac{k(\beta_0 s+\epsilon_0)}{\beta_0 s+\epsilon_0+k}\right\}v$$

$$=\gamma\frac{\mathrm{d}^2 v}{\mathrm{d}z^2}+\frac{kq_0}{\pi s(\beta_0 s+\epsilon_0+k)}\frac{1-e^{-s\zeta}}{1-e^{-s}}+\epsilon\int_{-l}^{l}v(\xi)B(\xi,z)\,\mathrm{d}\xi \qquad (15)$$

where $B(\xi,z)$ is the differential absorption factor between two ring elements at ξ and z. The analytical expression of $B(\xi,z)$ is given in Eq. (A1) in Appendix A. The detail of deriving Eq. (A1) is shown in the literature.[10]

For defining the solution of Eq. (15), one introduces the following boundary conditions showing that the tube ends are

insulated:

$$v'(\pm l)=0 \tag{16}$$

The variational principle is applicable to the boundary value problem in Eqs. (15) and (16). It is easily seen that an extremum of the following functional is equivalent to the solution satisfying Eq. (16):

$$J=\epsilon\int_{-l}^{l}\int_{-l}^{l}v(\xi)v(z)B(\xi,z)\mathrm{d}\xi\mathrm{d}z - \left\{\beta s+\epsilon+\frac{k(\beta_0 s+\epsilon_0)}{\beta_0 s+\epsilon_0+k}\right\}\int_{-l}^{l}v^2\mathrm{d}z - \gamma\int_{-l}^{l}\left(\frac{\mathrm{d}v}{\mathrm{d}z}\right)^2\mathrm{d}z+\frac{2kq_0}{\pi s(\beta_0 s+\epsilon_0+k)}\frac{1-e^{-s\zeta}}{1-e^{-s}}\int_{-l}^{l}v\mathrm{d}z \tag{17}$$

The Ritz procedure is instrumental in finding a better approximation of the extremum. In considering Eq. (16) and the axial symmetry about $z=0$, the following representation is employed as a test function:

$$v=(q_0/\pi)\{a(s)-b(s)(l^2z^2-z^4/2)\} \tag{18}$$

Substituting Eq. (18) into Eq. (17), one has a reduced expression of Eq. (17):

$$J=\left(\frac{q_0}{\pi}\right)^2\left\{-(g_{11}+2lw)a^2+2\left(g_{12}+\frac{7}{15}l^5w\right)ab - \left(g_{22}+\frac{107}{630}l^9w\right)b^2 + \frac{2k}{s(\beta_0 s+\epsilon_0+k)}\frac{1-e^{-s\zeta}}{1-e^{-s}}\left(2la-\frac{7}{15}l^5b\right)\right\} \tag{19}$$

where w is expressed as

$$w=\beta s+k(\beta_0 s+\epsilon_0)/(\beta_0 s+\epsilon_0+k) \tag{20}$$

The coefficients g_{11}, g_{12}, and g_{22} are given in Eq. (B1) in Appendix B.

The unknown parameters a and b are so determined as to minimize Eq. (19):

$$\frac{\partial J}{\partial a}=\frac{\partial J}{\partial b}=0 \tag{21}$$

This relation yields the following expressions:

$$a(s)=\frac{k(w+p_1)}{s(w+\Omega_1)(w+\Omega_2)(\beta_0 s+\epsilon_0+k)}\frac{1-e^{-s\zeta}}{1-e^{-s}}$$
$$b(s)=\frac{kp_2}{s(w+\Omega_1)(w+\Omega_2)(\beta_0 s+\epsilon_0+k)}\frac{1-e^{-s\zeta}}{1-e^{-s}} \tag{22}$$

where p_1 and p_2 are defined as

$$p_1=\frac{525}{32l^9}g_{22}-\frac{245}{64l^5}g_{12} \qquad p_2=\frac{525}{32l^9}g_{12}-\frac{245}{64l^5}g_{11} \tag{23}$$

The constants Ω_1 and Ω_2 are solutions to a quadratic equation satisfying the following relations:

$$\Omega_1+\Omega_2=\frac{525}{64l^9}\left(2g_{22}-\frac{14}{15}l^4g_{12}+\frac{107}{630}l^8g_{11}\right)$$
$$\Omega_1\Omega_2=\frac{525}{64l^{10}}(g_{11}g_{22}-g_{12}^2) \tag{24}$$

Applying the Laplace transform inversion to Eqs. (22) with respect to s, one finds the original functions of $a(s)$ and $b(s)$. Thus the following result is obtained:

$$u=\frac{k_0q_0\lambda_0}{\pi\epsilon_0\beta}[a_{11}\{P(\tau;\zeta)-R(\tau;\zeta,\omega_{11})\} +a_{12}\{P(\tau;\zeta)-R(\tau;\zeta,\omega_{12})\} +a_{21}\{P(\tau;\zeta)-R(\tau;\zeta,\omega_{21})\} +a_{22}\{P(\tau;\zeta)-R(\tau;\zeta,\omega_{22})\}] - \frac{k_0q_0\lambda_0p_2}{\pi\epsilon_0\beta^2}[b_{11}\{P(\tau;\zeta)-R(\tau;\zeta,\omega_{11})\} +b_{12}\{P(\tau;\zeta)-R(\tau;\zeta,\omega_{12})\} +b_{21}\{P(\tau;\zeta)-R(\tau;\zeta,\omega_{21})\} +b_{22}\{P(\tau;\zeta)-R(\tau;\zeta,\omega_{22})\}](l^2z^2-z^4/2) \tag{25}$$

where the function $R(\tau;\zeta,\omega)$ has the following form:

$$R(\tau;\zeta,\omega)=\sum_{m=0}^{\infty}\{\eta(\tau-m)e^{-\omega(\tau-m)}-\eta(\tau-m-\zeta)e^{-\omega(\tau-m-\zeta)}\} \tag{26}$$

The constants k_0 and λ_0 are defined as

$$k_0=\epsilon_0k/(\epsilon_0+k) \qquad \lambda_0=(\epsilon_0+k)/\beta_0 \tag{27}$$

Then the following relations give the definitions of ω_{11}, ω_{12}, ω_{21}, and ω_{22}:

$$\omega_{11}+\omega_{12}=(\Omega_1+k)/\beta+\lambda_0 \qquad \omega_{11}\omega_{12}=(\Omega_1+k_0)\lambda_0/\beta$$
$$\omega_{21}+\omega_{22}=(\Omega_2+k)/\beta+\lambda_0 \qquad \omega_{21}\omega_{22}=(\Omega_2+k_0)\lambda_0/\beta \tag{28}$$

The coefficients a_{11}, a_{12}, a_{21}, a_{22}, b_{11}, b_{12}, b_{21}, and b_{22} are given in Eqs. (B3) and (B4) of Appendix B.

Substitution of Eq. (25) into Eq. (14) leads to the infinite series which converge as m approaches infinity. The results are written as

$$u_{\substack{\max\\\min}}=\frac{k_0q_0}{\pi\epsilon_0}\left\{a_{\substack{\max\\\min}}-b_{\substack{\max\\\min}}\left(l^2z^2-\frac{z^4}{2}\right)\right\} \tag{29}$$

where $a_{\max}$, $a_{\min}$, $b_{\max}$, and $b_{\min}$ are given in Eqs. (B5) and (B6). If there is no eclipse in orbit ($\zeta=1$), then Eq. (29) is reduced to the following simple form:

$$u_\infty=\frac{k_0q_0}{\pi\epsilon_0(\Omega_1+k_0)(\Omega_2+k_0)}\left\{p_1+k_0-p_2\left(l^2z^2-\frac{z^4}{2}\right)\right\} \tag{30}$$

As mentioned before, the telescope contracts slightly during an eclipse. The following expression provides a theoretical means of estimating thermal contraction:

$$\mathrm{d}\Delta l=e_T(T_{\max}-T_{\min})\mathrm{d}z\approx(e_T/4\sigma\bar{T}^3)(u_{\max}-u_{\min})\mathrm{d}z \tag{31}$$

Integrating Eq. (31) over all such elements dz, one finds the total of axial contraction:

$$\Delta L=r\Delta l=\frac{k_0e_T\bar{T}rl}{4\zeta}\left\{(a_{\max}-a_{\min})-\frac{7}{30}l^4(b_{\max}-b_{\min})\right\} \tag{32}$$

Circumferential Temperature Distribution

For a relatively long space telescope, axial temperature gradients are so small that the temperature can be regarded as dependent on φ only. Equation (13) is then reduced to the

following expression:

$$\left\{\beta s+\epsilon+\frac{k(\beta_0 s+\epsilon_0)}{\beta_0 s+\epsilon_0+k}\right\}v$$
$$=\gamma\frac{d^2v}{d\varphi^2}+\frac{kq_0}{s(\beta_0 s+\epsilon_0+k)}\frac{1-e^{-s\zeta}}{1-e^{-s}}f_s(\varphi)$$
$$+\epsilon\int_0^{2\pi}v(\psi)B(\psi,\varphi)d\psi \tag{33}$$

where $B(\psi,\varphi)$ is the differential absorption factor between two narrow longitudinal area elements at ψ and φ. The analytical expression of $B(\psi,\varphi)$ is given in Eq. (C1) in Appendix C. The derivation of Eq. (C1) is also presented in the literature.[10]

Now attention is turned to such periodicity as $u(\varphi+2\pi)=u(\varphi)$. This suggests that the Fourier series expansion technique tried by Katzoff[7] is instrumental in solving Eq. (33). Therefore, the variable is placed in the following cosine series in φ:

$$v=q_0\sum_{n=0}^{\infty}a_n(s)\cos n\varphi \tag{34}$$

Equation (4) is also expanded in a Fourier cosine series:

$$f_s(\varphi)=\sum_{n=0}^{\infty}A_n\cos n\varphi \tag{35}$$

where A_n is expressed as

$$A_0=1/\pi \qquad A_1=1/2$$

$$A_n=\begin{cases}\dfrac{2}{\pi}\dfrac{(-1)^{n/2-1}}{n^2-1} & (n=2,4,6,\ldots)\\ 0 & (n=3,5,7,\ldots)\end{cases} \tag{36}$$

Substituting Eqs. (34) and (35) into Eq. (33), one finds a closed-form expression of the unknown coefficient $a_n(s)$:

$$a_n(s)=\frac{kA_n}{\beta_0\beta s(s+\omega_{1n})(s+\omega_{2n})}\frac{1-e^{-s\zeta}}{1-e^{-s}} \tag{37}$$

where ω_{1n} and ω_{2n} are solutions of a quadratic equation satisfying the following relations:

$$\omega_{1n}+\omega_{2n}=\left(k+\gamma n^2+\frac{\epsilon n^2}{n^2-\mu^2}\right)\beta^{-1}+\lambda_0$$

$$\omega_{1n}\omega_{2n}=\lambda_0\left(k_0+\gamma n^2+\frac{\epsilon n^2}{n^2-\mu^2}\right)\beta^{-1} \tag{38}$$

The Laplace transform inversion of Eq. (37) with respect to s results in the circumferential temperature distribution at any time τ:

$$u=\frac{k_0q_0\lambda_0}{\epsilon_0\beta}\sum_{n=0}^{\infty}\frac{A_n}{\omega_{2n}-\omega_{1n}}\left[\frac{1}{\omega_{1n}}\{P(\tau;\zeta)-R(\tau;\zeta,\omega_{1n})\}\right.$$
$$\left.+\frac{1}{\omega_{2n}}\{P(\tau;\zeta)-R(\tau;\zeta,\omega_{2n})\}\right]\cos n\varphi \tag{39}$$

The calculus shown in Eq. (14) with Eq. (39) amounts to finding the limits of geometrical progressions. After some manipulation, the final results are obtained:

$$u_{\substack{\max\\ \min\\ \infty}}=\frac{k_0q_0}{\epsilon_0}\sum_{n=0}^{\infty}a_{n\,\substack{\max\\ \min\\ \infty}}\cos n\varphi \tag{40}$$

where $a_{n\,\max}$, $a_{n\,\min}$, and $a_{n\infty}$ are given by

$$a_{n\,\max}=\frac{\lambda_0A_n}{\beta(\omega_{2n}-\omega_{1n})}\left(\frac{1}{\omega_{1n}}\frac{1-e^{-\omega_{1n}\zeta}}{1-e^{-\omega_{1n}}}-\frac{1}{\omega_{2n}}\frac{1-e^{-\omega_{2n}\zeta}}{1-e^{-\omega_{2n}}}\right)$$
$$a_{n\,\min}=\frac{\lambda_0A_n}{\beta(\omega_{2n}-\omega_{1n})}\left(\frac{1}{\omega_{1n}}\frac{e^{-\omega_{1n}(1-\zeta)}-e^{-\omega_{1n}}}{1-e^{-\omega_{1n}}}\right.$$
$$\left.-\frac{1}{\omega_{2n}}\frac{e^{-\omega_{2n}(1-\zeta)}-e^{-\omega_{2n}}}{1-e^{-\omega_{2n}}}\right)$$
$$a_{n\infty}=A_n\left(k_0+\gamma n^2+\frac{\epsilon n^2}{n^2-\mu^2}\right)^{-1} \tag{41}$$

The infinite series in Eq. (40) converge rapidly, and thereby the higher than fourth-order terms ($n>4$) may be disregarded for engineering calculations.

Seeing that booms are usually not thermally insulated, they can be treated as uninsulated cylinders of long length and thin wall. Therefore, the thermal behavior of a boom of seamless fabrication is predictable from the above analytical results for no insulation. Since the uninsulated surface is specified as $k=\infty$ and $\beta_0=0$, Eq. (37) reduces to the following representation:

$$a_n(s)=\frac{A_n}{\beta s(s+\omega_n)}\frac{1-e^{-s\zeta}}{1-e^{-s}} \tag{42}$$

where ω_n is written as

$$\omega_n=\left(\epsilon_0+\gamma n^2+\frac{\epsilon n^2}{n^2-\mu^2}\right)\beta^{-1} \tag{43}$$

The Laplace transform inversion of Eq. (42) with respect to s leads to an expression corresponding to Eq. (39):

$$u=\frac{q_0}{\beta}\sum_{n=0}^{\infty}\frac{A_n}{\omega_n}\{P(\tau;\zeta)-R(\tau;\zeta,\omega_n)\}\cos n\varphi \tag{44}$$

Equation (14) is also applicable to finding the maximum and minimum temperature distributions of the boom in a quasisteady state, which have the same form as obtained by putting $k=\infty$ in Eq. (40):

$$u_{\substack{\max\\ \min\\ \infty}}=q_0\sum_{n=0}^{\infty}a_{n\,\substack{\max\\ \min\\ \infty}}\cos n\varphi \tag{45}$$

The coefficients $a_{n\,\max}$, $a_{n\,\min}$, and $a_{n\infty}$ are here expressed in simpler forms than Eqs. (41):

$$a_{n\,\max}=\frac{A_n}{\beta\omega_n}\frac{1-e^{-\omega_n\zeta}}{1-e^{-\omega_n}} \qquad a_{n\,\min}=\frac{A_n}{\beta\omega_n}\frac{e^{-\omega_n(1-\zeta)}-e^{-\omega_n}}{1-e^{-\omega_n}}$$
$$a_{n\infty}=A_n\left(\epsilon_0+\gamma n^2+\frac{\epsilon n^2}{n^2-\mu^2}\right)^{-1} \tag{46}$$

Circumferential Heat Pipes

The use of heat pipes was first proposed by Katzoff[7,8] to equalize the wall temperatures of a large space telescope. In this connection, he presented typical examples showing the usefulness of isothermalizer heat pipes. But the applicability of his approach is limited to a few specific cases. The present

analysis is performed with a view toward obtaining results which can be applied more widely. As a model of space telescopes, one considers an uninsulated cylinder ($k=\infty$) to which circumferential heat pipes shaping simple hoops are mounted at such regular intervals as $Z=W, 3W,\ldots, (2N-1)W$. Here the integer N denotes the number of heat pipes and satisfies the relation $L=2NW$.

If the length is sufficiently long and the heat pipes function normally, then the relation $T(W\pm Z)\approx T(3W\pm Z)\approx \ldots \approx T((2N-1)W\pm Z)$ holds for $0\le Z\le W$. This shows that one has to consider only the temperature profile in the interval $(2n-1)W\le Z\le 2nW$. For simplicity, one introduces the new dimensionless distance which takes the place of the first expression of Eq. (1):

$$z=Z/W \tag{47}$$

But the new origin ($z=0$) is put at the nth heat pipe ($Z=(2n-1)W$). The interval mentioned above is thereby rewritten as $0\le z\le 1$, in which the governing equation will be set up.

For facilitating the analysis, it is assumed that the telescope is in an orbit with no eclipse ($\zeta=1$), that is, in a steady state. Providing that $k=\infty$ and $\zeta=1$, Eqs. (2) are changed into the following integrodifferential equation describing the heat balance of such a telescope:

$$\lambda h\left(\frac{1}{r^2}\frac{\partial^2 T}{\partial\varphi^2}+\frac{1}{W^2}\frac{\partial^2 T}{\partial z^2}\right)$$

$$=(\epsilon_0+\epsilon)\sigma T^4-\epsilon\int_0^1\int_0^{2\pi}\sigma T^4(\xi,\psi)B(\xi,\psi;z,\varphi)\,\mathrm{d}\xi\mathrm{d}\psi-q_0 f_s(\varphi) \tag{48}$$

In solving Eq. (48), the following conditions should be taken into consideration:

$$\int_0^{2\pi}\left(\frac{\partial T}{\partial z}\right)_{z=0}\mathrm{d}\varphi=0 \qquad \left(\frac{\partial T}{\partial z}\right)_{z=1}=0 \qquad T(0,\varphi)=\bar{T} \tag{49}$$

In Eq. (49), the first expression shows that the heat influx from the sunlit portion is transferred to the shaded portion with the heat pipe placed at $z=0$. Then the second expression shows that the temperature gradient should be smooth at $z=1$ as well as at other points. The third expression of Eq. (49) results from the fact that heat pipes can be regarded as isothermal. The reference temperature $\bar{T}$ is here given by the expression derived from Eq. (8) with $\zeta=1$:

$$\bar{T}=(q_0/\pi\epsilon_0\sigma)^{1/4} \tag{50}$$

Since it is very difficult to solve Eq. (48) associated with Eq. (49), the assumption is made that the solution has the following form:

$$T(z,\varphi)=\bar{T}[1-(3/2)c\{1-\pi f_s(\varphi)\}(2z-z^2)] \tag{51}$$

It is apparent that Eq. (51) satisfies Eq. (49). By taking the average over the whole interval $0\le z\le 1$, Eq. (48) is simplified as

$$\lambda h\left\{\frac{1}{r^2}\frac{\mathrm{d}^2 T_B}{\mathrm{d}\varphi^2}+\frac{3(\bar{T}-T_B)}{W^2}\right\}$$

$$=(\epsilon_0+\epsilon)\sigma T_B^4-\epsilon\int_0^{2\pi}\sigma T_B^4(\psi)B(\psi,\varphi)\,\mathrm{d}\psi-q_0 f_s(\varphi) \tag{52}$$

The new variable T_B is so defined here as to give the mean temperature distribution:

$$T_B\equiv\int_0^1 T(z,\varphi)\,\mathrm{d}z=\bar{T}\theta \tag{53}$$

where θ is expressed as

$$\theta=1-c\{1-\pi f_s(\varphi)\} \tag{54}$$

The problem is now attributed to determining the unknown coefficient c.

In order to find an analytical solution of Eq. (52), the following approximation is employed:

$$T_B^4\approx 4\bar{T}^4(\theta-3/4) \tag{55}$$

Thus Eq. (52) is linearized as

$$\gamma\frac{\mathrm{d}^2\theta}{\mathrm{d}\varphi^2}=(\gamma'+\epsilon_0+\epsilon)\theta-\epsilon\int_0^{2\pi}\theta(\psi)B(\psi,\varphi)\,\mathrm{d}\psi$$

$$-\frac{\pi\epsilon_0}{4}f_s(\varphi)-\left(\gamma'+\frac{3}{4}\epsilon_0\right) \tag{56}$$

where γ' is defined as

$$\gamma'=3\gamma(r/W)^2 \tag{57}$$

For convenience of mathematical treatments, Eq. (56) is replaced with the following functional

$$J=\gamma\int_0^{2\pi}\left(\frac{\mathrm{d}\theta}{\mathrm{d}\varphi}\right)^2\mathrm{d}\varphi+(\gamma'+\epsilon_0+\epsilon)\int_0^{2\pi}\theta^2\mathrm{d}\varphi$$

$$-\epsilon\int_0^{2\pi}\int_0^{2\pi}\theta(\psi)\theta(\varphi)B(\psi,\varphi)\,\mathrm{d}\psi\mathrm{d}\varphi$$

$$-\frac{\pi\epsilon_0}{2}\int_0^{2\pi}\theta(\varphi)f_s(\varphi)\,\mathrm{d}\varphi-2\left(\gamma'+\frac{3}{4}\epsilon_0\right)\int_0^{2\pi}\theta\mathrm{d}\varphi \tag{58}$$

Substituting Eq. (54) into Eq. (58), one has the following representation:

$$\frac{J}{\pi}=\left[\gamma\pi^2+(\gamma'+\epsilon_0)(\pi^2-4)\right.$$

$$\left.+\epsilon\left\{\frac{\pi^2}{1-\mu^2}-\frac{2\pi\mu}{(1-\mu^2)^2}\cot\frac{\pi\mu}{2}\right\}\right]\frac{c^2}{2}$$

$$-\frac{\epsilon_0}{4}(\pi^2-4)c-2(\gamma'+\epsilon_0) \tag{59}$$

The coefficient c is determined in such a way that $\mathrm{d}J/\mathrm{d}c=0$:

$$c=\frac{\epsilon_0}{4}(\pi^2-4)\left[\gamma\pi^2+(\gamma'+\epsilon_0)(\pi^2-4)\right.$$

$$\left.+\epsilon\left\{\frac{\pi^2}{1-\mu^2}-\frac{2\pi\mu}{(1-\mu^2)^2}\cot\frac{\pi\mu}{2}\right\}\right]^{-1} \tag{60}$$

The results computed from Eqs. (53, 54, and 60) were compared with the numerical examples given by Katzoff[8] to evalute the error caused by the approximations employed here. It is concluded that the accuracy is good because the difference between the two remains less than 5 K for the two cases specified as $\epsilon=0.0$ and 1.0.

Thermomechanical Analysis of Booms

Circumferential Temperature Distribution

Figure 1 shows a cross section of a boom with locked seams. As shown, the cross section may be oriented in such a way that the path from the outer seam to the inner seam is traced by counterclockwise or clockwise rotation of the radius vector. The coordiante system is defined in the figure with the

solar direction. In this system, the z axis is the centroidal axis and the z coordinate expresses the longitudinal distance measured from the root at which the boom is clamped. The x axis is the mass symmetry axis which bisects the overlapped sector specifed by the angle ϕ. The angle ϕ' is hereafter substituted for ϕ:

$$\phi' = 2\pi + \phi \tag{61}$$

The y axis is normal to the x axis in the cross-sectional plane and displaced from the geometrical center by the distance $-(2r/\phi')\sin(\phi'/2)$. The outer edge of the overlapped portion is defined as $\varphi = 0$, and the angles φ and φ_s are measured from it in the direction shown in Fig. 1.

In most cases, torsional rigidity of booms is enhanced by the use of seams of interlocking tabs.[3] This implies that torsional displacements are absent. It is, therefore, permissible to assume that the overlapped sector does not vary along the length. Furthermore, it is assumed that thermal bending has an insignificant effect on the form of the solar heat input function. It follows that the temperature is independent of the longitudinal location. As seen from Fig. 1, only the outer seam ($0 \le \varphi \le 2\pi$) can receive the solar radiation and emit infrared radiation to space. In the overlapped portion ($0 \le \varphi \le \phi$), the outer seam does not contribute to the internal radiation exchange. The interradiation takes place in the interior of the inner seam ($\phi \le \varphi \le \phi'$). In addition to such radiation heat transfer, there exists the circumferential heat conduction which occurs in every part of the seam ($0 \le \varphi \le \phi'$). It is then assumed that there is no thermal interchange across the gap of the overlapped sector.

From the above assumptions and descriptions, it is now possible to set up the governing equation. But the solar elevation angle θ_s shown in Fig. 1 is no longer constant, because a boom will always point approximately toward the center of the Earth. However, the time variability of the solar direction makes the analysis formidably complicated. For this reason, as in the foregoing analyses,[1-4] the assumption is also made that the solar heat input does not change during the sunlit part of orbit. Thus one obtains the following integrodifferential equation with the condition that there is no eclipse in the orbit:

$$\frac{\lambda h}{r^2}\frac{d^2T}{d\varphi^2} + q_0 f_s(\varphi;\varphi_s)\eta(2\pi-\varphi) - \epsilon_0\sigma T^4\eta(2\pi-\varphi) - \epsilon\sigma T^4\eta(\varphi-\phi) + \epsilon\eta(\varphi-\phi)\int_\phi^{\phi'}\sigma T^4(\psi)B(\psi,\varphi)\,d\psi = 0 \tag{62}$$

The solar heat input function $f_s(\varphi;\varphi_s)$ is here defined as follows:

1) The overlapped portion is not illuminated, $\pi/2 \le \varphi_s \le 3\pi/2$:

$$f_s(\varphi;\varphi_s) = \begin{cases} \cos(\varphi-\varphi_s) & \text{if} \quad \varphi_s - \dfrac{\pi}{2} \le \varphi \le \varphi_s + \dfrac{\pi}{2} \qquad (63a) \\ 0 & \text{if} \quad 0 \le \varphi \le \varphi_s - \dfrac{\pi}{2} \quad \text{or} \quad \varphi_s + \dfrac{\pi}{2} \le \varphi \le 2\pi \qquad (63b) \end{cases}$$

2) The overlapped portion is illuminated such that $0 \le \varphi_s < \pi/2$:

$$f_s(\varphi;\varphi_s) = \begin{cases} \cos(\varphi-\varphi_s) & \text{if} \quad 0 \le \varphi \le \varphi_s + \dfrac{\pi}{2} \quad \text{or} \quad \varphi_s + \dfrac{3\pi}{2} \le \varphi \le 2\pi \qquad (63c) \\ 0 & \text{if} \quad \varphi_s + \dfrac{\pi}{2} \le \varphi \le \varphi_s + \dfrac{3\pi}{2} \qquad (63d) \end{cases}$$

3) The overlapped portion is illuminated such that $3\pi/2 < \varphi_s \le 2\pi$:

$$f_s(\varphi;\varphi_s) = \begin{cases} \cos(\varphi-\varphi_s) & \text{if} \quad 0 \le \varphi \le \varphi_s - \dfrac{3\pi}{2} \quad \text{or} \quad \varphi_s - \dfrac{\pi}{2} \le \varphi \le 2\pi \qquad (63e) \\ 0 & \text{if} \quad \varphi_s - \dfrac{3\pi}{2} \le \varphi \le \varphi_s - \dfrac{\pi}{2} \qquad (63f) \end{cases}$$

By using the first expression of Eq. (5) and the second expression of Eq. (7), Eq. (62) is linearized as

$$\gamma\frac{d^2u}{d\varphi^2} + q_0 f_s(\varphi;\varphi_s)\eta(2\pi-\varphi) - \epsilon_0 u\eta(2\pi-\varphi) - \epsilon u\eta(\varphi-\phi) + \epsilon\eta(\varphi-\phi)\int_\phi^{\phi'} u(\psi)B(\psi,\varphi)\,d\psi = 0 \tag{64}$$

where γ is given by the third expression of Eq. (10) but $\bar{T}$ is expressed as in Eq. (50). Since the edge heat losses are negligible, the boundary conditions may be taken as $T'(0) = T'(\phi') = 0$. This relation is rewritten as

$$u'(0) = u'(\phi') = 0 \tag{65}$$

The boundary value problem defined in Eqs. (64) and (65) is reducible to the following functional

$$J = \epsilon\int_\phi^{\phi'}\int_\phi^{\phi'} u(\psi)u(\varphi)B(\psi,\varphi)\,d\psi\,d\varphi - \epsilon_0\int_0^{2\pi} u^2\,d\varphi - \epsilon\int_\phi^{\phi'} u^2\,d\varphi - \gamma\int_0^{\phi'}\left(\frac{du}{d\varphi}\right)^2 d\varphi + 2q_0\int_0^{2\pi} f_s(\varphi;\varphi_s)u(\varphi)\,d\varphi \tag{66}$$

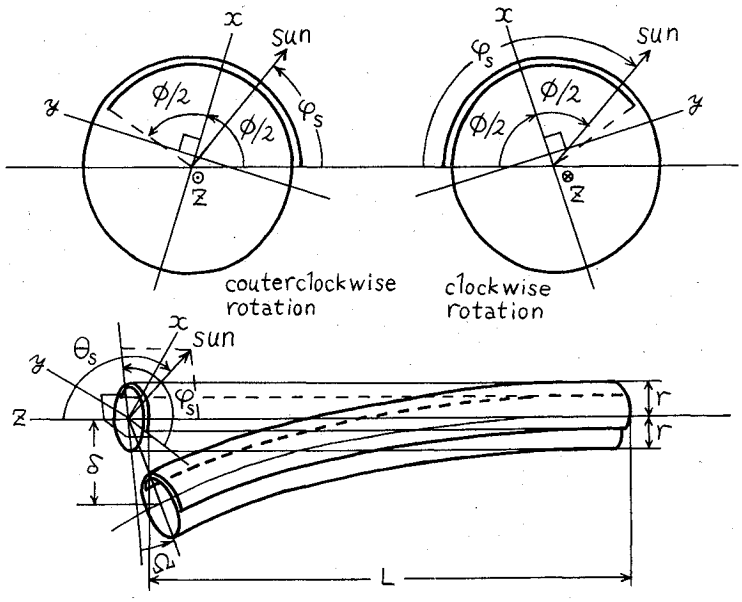

Fig. 1 Mathematical model and coordinate system.

The Ritz procedure is employed as a means of obtaining an analytical solution of Eq. (64). According to the test results presented by Florio and Hobbs,[2] the circumferential temperature distributions seem to be biquadratic. In considering this fact and Eq. (65), the following representation is chosen here as a test function:

$$u=q_0\left\{a+b\left(\frac{\varphi^4}{4}-\frac{\phi'\varphi^3}{3}\right)-c\left(\frac{\varphi^3}{3}-\frac{\phi'\varphi^2}{2}\right)\right\} \tag{67}$$

The integrations in Eq. (66) are performed by using Eq. (67), and the result is arranged as

$$J/q_0^2=-(f_{11}a^2-2f_{12}ab+2f_{13}ac+f_{22}b^2-2f_{23}bc+f_{33}c^2)+2(2a-K_2b+K_3c) \tag{68}$$

where f_{11}, f_{12}, f_{13}, f_{22}, f_{23}, and f_{33} are given in Eq. (D1) of Appendix D. Then the coefficients K_2 and K_3 are defined as in Eq. (D6). The unknown coefficients a, b, and c are determined from the following relation:

$$\frac{\partial J}{\partial a}=\frac{\partial J}{\partial b}=\frac{\partial J}{\partial c}=0 \tag{69}$$

The simultaneous linear equations resulted from Eq. (69) yield the following expressions:

$$a=\{2(f_{23}^2-f_{22}f_{33})+K_2(f_{12}f_{33}-f_{13}f_{23})+K_3(f_{13}f_{22}-f_{12}f_{23})\}D^{-1} \tag{70a}$$

$$b=\{2(f_{13}f_{23}-f_{12}f_{33})+K_2(f_{11}f_{33}-f_{13}^2)+K_3(f_{12}f_{13}-f_{11}f_{23})\}D^{-1} \tag{70b}$$

$$c=\{2(f_{13}f_{22}-f_{12}f_{23})+K_2(f_{11}f_{23}-f_{12}f_{13})+K_3(f_{12}^2-f_{11}f_{22})\}D^{-1} \tag{70c}$$

where D is given by

$$D=f_{11}f_{23}^2+f_{22}f_{13}^2+f_{33}f_{12}^2-f_{11}f_{22}f_{33}-2f_{12}f_{13}f_{23} \tag{71}$$

Solar Deflection

The unsymmetric temperature distribution given by Eq. (67) causes longitudinal thermal stresses due to the difference in the relative expansion of longitudinal area elements. They are expressed in the following form in accordance with Hooke's law on thermoelasticity:

$$\sigma_z=Ge_TT \tag{72}$$

In considering Eq. (50) and the first expression of Eq. (5), Eq. (72) is approximated as

$$\sigma_z\approx Ge_T\bar{T}(3/4+u/4\sigma\bar{T}^4) \tag{73}$$

Based upon the coordinate system shown in Fig. 1, the thermal bending moments are represented by the following integrals performed on an area element $da=hrd\varphi$:

$$M_x=\int y\sigma_z da \qquad M_y=-\int x\sigma_z da \tag{74}$$

The integrations are taken over the entire cross-sectional area. Then the coordinates x and y indicate a point around the cross-sectional perimeter and, hence, are expressed as

$$x=r\left\{\frac{2}{\phi'}\sin\frac{\phi'}{2}-\cos\left(\varphi-\frac{\phi'}{2}\right)\right\} \qquad y=-r\sin\left(\varphi-\frac{\phi'}{2}\right) \tag{75}$$

The use of Eqs. (73) and (75) associated with Eq. (67) leads to a reduced expression of Eq. (74):

$$M_x=\frac{q_0 G e_T h r^2}{4\sigma\bar{T}^3}m_x \qquad M_y=-\frac{q_0 G e_T h r^2}{4\sigma\bar{T}^3}m_y \tag{76}$$

where m_x and m_y are given by

$$m_x=(2c-b\phi')\left\{\phi'\left(1+\frac{\phi'^2}{12}\right)\cos\frac{\phi'}{2}-2\sin\frac{\phi'}{2}\right\}$$

$$m_y=b\left\{6\phi'\cos\frac{\phi'}{2}+\left(\frac{\phi'^4}{60}+\phi'^2-12\right)\sin\frac{\phi'}{2}\right\} \tag{77}$$

The deflection induced by the thermal bending is obtainable from the Bernoulli-Euler equation for a cantilevered element. If the square of the slope of the deflected shape is small compared to unity, the equation can be simplified to the extent of merely including a second-order differential derivative term. The deflected shape then becomes parabolic. This results in the following expression for the boom tip deflections in the positive x and positive y directions:

$$\delta_x=M_y L^2/2GI_y \qquad \delta_y=-M_x L^2/2GI_x \tag{78}$$

where I_x and I_y are the geometrical moments of inertia of the cross section:

$$I_x=\int y^2 da \qquad I_y=\int x^2 da \tag{79}$$

Because of Eq. (75), Eq. (79) reduces to the following form:

$$I_x=hr^3 i_x \qquad I_y=hr^3 i_y \tag{80}$$

where i_x and i_y are given by

$$i_x=\frac{\phi'}{2}-\frac{\sin\phi'}{2} \qquad i_y=\frac{\phi'}{2}+\frac{\sin\phi'}{2}-\frac{4}{\phi'}\sin\frac{\phi'}{2} \tag{81}$$

Equations (81) are the same as given by Eby and Karam.[3] The boom tip deflections are readily obtained by substituting Eqs. (76) and (80) into Eq. (78):

$$\delta_x=-\frac{q_0 e_T L^2}{8\sigma\bar{T}^3 r}\frac{m_y}{i_y} \qquad \delta_y=-\frac{q_0 e_T L^2}{8\sigma\bar{T}^3 r}\frac{m_x}{i_x} \tag{82}$$

Since the solar deflection is not generally aligned with the solar direction, the out-of-sunline angle defined as follows provides a measure of the displacement from the solar vector:

$$\Omega=\tan^{-1}\left(\frac{m_x i_y}{m_y i_x}\right)-\left(\varphi_s-\frac{\phi}{2}+\pi\right) \tag{83}$$

Based upon the small deflection theory, the method developed for a boom of locked seams is also applicable to estimation of solar deflections of a boom of seamless fabrication. In other words, one may employ Eqs. (73), (74), (78), and (79) as before. But, Eq. (73) needs to be evaluated by using Eqs. (45) and (8). Furthermore, in Eqs. (74) and (79), the following expressions should be substituted for Eq. (75):

$$x=r\cos\varphi \qquad y=r\sin\varphi \tag{84}$$

As a result of computations based upon Eqs. (45) and (84), one has the following representations:

$$M_x=0 \qquad M_y=-\frac{q_0 G e_T h r^2}{4\sigma\bar{T}^3}\pi a_1 \tag{85}$$

$$I_x=I_y=\pi hr^3 \tag{86}$$

Substituting Eqs. (85) and (86) into Eq. (78), one finds the result different from Eq. (82):

$$\delta_x=-\frac{q_0 e_T L^2}{8\sigma\bar{T}^3 r}a_1 \qquad \delta_y=0 \tag{87}$$

Equation (87) shows that any coefficients in Eq. (45) other than a_1 have no effect on the solar deflection of booms of seamless fabrication.

Numerical Results and Discussions

One practical application of the analytical results for an insulated cylinder is the estimation of wall temperature distributions of a space telescope. Telescopes discussed here have a 150 cm radius and 1.0 mm wall thickness. The wall is made of aluminum specified as $C=0.92$ J/g·K, $\rho=2.70$ g/cm^3, $\lambda=2.10$ W/cm·K, and $e_T=2.27\times10^{-5}$/K, and wrapped in aluminized Mylar sheets specified as $C_0=0.84$ J/g·K and $\rho_0=1.24\times10^{-4}$ g/cm^2. Tables 1 and 2 show the results of parametric studies made to evaluate the effects of multilayer insulation and surface properties on the temperature gradient. The results for a telescope with a large length-to-diameter ratio ($l\gg1$) are given in Table 1, and those for a 9 m telescope ($l=6.0$) in Table 2. The values of parameters k, N_0, α_0, ϵ_0, and ϵ are the same as those investigated by Katzoff[7] and cover a whole range of interest. The computations have been carried out on the condition that the telescope is in a 100 min orbit with an eclipse of 40% ($\zeta=0.60$) and with its axis normal ($\theta_s=90$ deg) to the solar radiation of one solar constant ($I_s=1.4$ kW/m^2).

The thermal behavior of the telscope in a quasisteady state is predictable from Tables 1 and 2. The rows designated as max and min indicate the maximum and minimum temperatures at the subsolar point ($\varphi=0$ deg) and at the antisolar point ($\varphi=180$ deg), and those at the closed end ($z=0.0$) and at the open end ($z=6.0$), respectively. The rows designated as CHP are added in Table 1 to show the degree of temperature uniformity attainable by employing isothermalizer heat pipes. The computations are made here with the condition that circumferential heat pipes are mounted on the structural tube at regular intervals of 20 cm. It is clearly seen from Table 1 that the heat pipes serve to isothermalize the telescope. In Table 2, the thermal contractions are listed in the rows designated as ΔL.

As expected, the multilayer insulation greatly helps to achieve temperature uniformity and constancy. In particular, it serves as a means of diminishing the temperature drop due to an eclipse in orbit. The comparison between the results for a 25-layer insulation and those for a 10-layer insulation shows that the number of layers makes no great difference in circumferential temperature gradients but has a considerable effect on thermal contractions. It is also seen that the temperature level is principally affected by the outer surface properties, α_0 and ϵ_0, and that it is almost independent of the inner surface properties, ϵ and τ_S. However, highly specular surfaces ($\tau_S=1.0$) contribute in a small degree to the temperature equalization. From Table 2, one finds that the thermal contractions are not influenced by the inner surface

Table 1 Wall temperatures (in K) at subsolar and antisolar points of space telescope

		$k=$	0.0010						0.0025			
		$N_0=$	25						10			
		$\alpha_0=$	0.40		0.25		0.15		0.40		0.25		0.15	
		$\epsilon_0=$	0.40		0.85		0.85		0.40		0.85		0.85	
		$\epsilon=$	0.20	0.90	0.20	0.90	0.20	0.90	0.20	0.90	0.20	0.90	0.20	0.90
State	φ, deg	$\tau_S=$	1.0	0.0	1.0	0.0	1.0	0.0	1.0	0.0	1.0	0.0	1.0	0.0
Max	0		263.0	262.4	193.4	193.2	170.2	170.0	264.3	262.9	194.1	193.4	170.7	170.2
	180		261.8	262.1	192.8	193.0	169.7	169.8	261.4	262.2	192.5	192.9	169.4	169.8
Min	0		262.2	261.9	193.2	193.0	170.0	169.9	262.5	261.7	193.5	192.9	170.3	169.9
	180		261.8	261.9	192.8	192.9	169.7	169.8	261.3	261.7	192.5	192.9	169.4	169.8

		$k=$	∞											
		$N_0=$	0											
		$\alpha_0=$	0.40				0.25				0.15			
		$\epsilon_0=$	0.40				0.85				0.85			
		$\epsilon=$	0.20		0.90		0.20		0.90		0.20		0.90	
State	φ, deg	$\tau_S=$	0.0	1.0	0.0	1.0	0.0	1.0	0.0	1.0	0.0	1.0	0.0	1.0
Max			363.4	363.1	328.0	327.5	272.5	272.4	253.0	252.6	234.7	234.6	219.4	219.0
	18ι		216.0	217.0	270.4	271.2	134.3	135.0	183.5	184.4	115.4	116.0	156.6	157.4
Min	0		219.2	218.9	197.1	197.1	182.7	182.5	158.1	157.9	177.5	177.3	155.6	155.3
	180		180.2	180.8	196.8	196.6	122.0	122.5	150.4	150.7	111.8	112.3	142.0	142.3
CHP	0		317.3	317.3	313.0	312.9	232.2	232.2	230.8	230.8	201.1	201.1	200.5	200.5
	180		288.6	288.6	290.6	290.7	213.2	213.2	213.9	213.9	189.2	189.2	189.5	189.5

Table 2 Wall temperatures (in K) at both ends of space telescope

		$k=$	0.0010											
		$N_0=$	25											
		$\alpha_0=$	0.40				0.25				0.15			
		$\epsilon_0=$	0.40				0.85				0.85			
		$\epsilon=$	0.20		0.90		0.20		0.90		0.20		0.90	
State	z	$\tau_S=$	0.0	1.0	0.0	1.0	0.0	1.0	0.0	1.0	0.0	1.0	0.0	1.0
Max	0.0		109.5	103.1	105.8	105.0	79.4	74.8	76.6	76.0	69.4	65.5	67.0	66.5
	6.0		73.9	95.3	86.2	86.2	68.4	69.2	62.4	62.4	60.1	60.8	54.7	54.7
Min	0.0		105.7	98.6	101.5	100.6	78.3	73.5	75.4	74.8	68.8	64.7	66.3	65.7
	6.0		87.9	89.5	78.9	78.9	66.6	67.5	60.1	60.0	59.1	59.8	53.3	53.3
ΔL,mm			0.0518	0.0518	0.0509	0.0509	0.0153	0.0153	0.0152	0.0152	0.0091	0.0091	0.0091	0.0091

		$k=$	0.0025											
		$N_0=$	10											
		$\alpha_0=$	0.40				0.25				0.15			
		$\epsilon_0=$	0.40				0.85				0.85			
		$\epsilon=$	0.20		0.90		0.20		0.90		0.20		0.90	
State	z	$\tau_S=$	0.0	1.0	0.0	1.0	0.0	1.0	0.0	1.0	0.0	1.0	0.0	1.0
Max	0.0		136.4	128.6	132.0	131.1	98.9	93.4	95.6	94.9	86.5	81.8	83.6	83.0
	6.0		117.2	119.0	107.7	107.7	85.3	86.4	77.9	77.9	75.1	75.9	68.3	68.3
Min	0.0		131.5	122.8	126.5	125.3	97.5	91.6	94.0	93.3	85.6	80.8	82.7	82.0
	6.0		109.5	111.6	98.3	98.3	83.1	84.3	75.0	75.0	73.7	74.6	66.5	66.5
ΔL, mm			0.1297	0.1297	0.1275	0.1275	0.0385	0.0385	0.0383	0.0383	0.0230	0.0230	0.0230	0.0230

Table 3 Effect of inner surface emittance on solar deflection

		φ_s, deg =	0	30	60	90	120	150	180	210	240	270	300	3
$\epsilon=0.0$	δ_x, cm		−48.5	−88.9	−99.3	−74.7	−32.6	8.3	43.0	68.1	81.1	80.7	56.2	6
	δ_y, cm		6.2	−17.7	−34.2	−35.6	−27.0	−16.7	−5.0	7.6	20.9	34.4	39.2	28
	δ, cm		48.9	90.6	105.0	82.8	42.4	18.6	43.3	68.6	83.7	87.7	68.5	28
	Ω, deg		67.8	56.3	34.0	10.5	−5.3	41.3	68.3	51.4	29.5	8.1	−10.1	1
$\epsilon=0.20$	δ_x, cm		−46.8	−88.5	−100.1	−76.3	−34.3	6.5	41.6	67.3	81.1	82.0	58.5	9
	δ_y, cm		5.5	−17.5	−33.2	−34.5	−26.0	−15.8	−4.4	7.8	20.5	33.3	37.7	26
	δ, cm		47.2	90.2	105.5	83.7	43.0	17.1	41.8	67.7	83.7	88.5	69.6	28
	Ω, deg		68.3	56.2	33.4	9.3	−7.9	37.5	68.9	51.6	29.2	7.1	−12.2	−3
$\epsilon=0.90$	δ_x, cm		−41.4	−86.4	−101.8	−80.2	−39.2	1.3	36.9	64.0	80.5	85.1	64.9	16
	δ_y, cm		3.4	−16.9	−30.4	−30.8	−22.6	−13.1	−2.6	8.2	19.2	30.0	33.0	22
	δ, cm		41.5	88.0	106.2	85.9	45.2	13.1	36.9	64.6	82.8	90.2	72.8	27
	Ω, deg		70.4	56.1	31.6	6.0	−15.1	20.7	70.9	52.3	28.4	4.4	−18.0	−20

properties but decrease with the absorptance to emittance ratio α_0/ϵ_0.

For a better understanding of the thermal behavior of a boom in space, a computation has been made for various angles of solar incidence under the condition that $I_s = 1.4$ kW/m^2 and $\theta_s = 90$ deg. The boom discussed here is a typical beryllium-copper rod with a 30.5 m length, a 0.635 mm radius, a 0.0381 mm thickness, and a seam overlapped for an angle of 150 deg. With reference to the thermal properties of beryllium copper, the wall material is defined as $\lambda = 1.06$ W/cm·K and $e_T = 1.66 \times 10^{-5}$/K. The exterior surface is then assumed to be plated with silver such that $\alpha_0 = 0.10$ and $\epsilon_0 = 0.06$. These data are the same as employed by Eby and Karam[3] which were used with a view to verifying the method of solution. The principal results of parametric studies are summarized in Table 3 and Figs. 2 and 3.

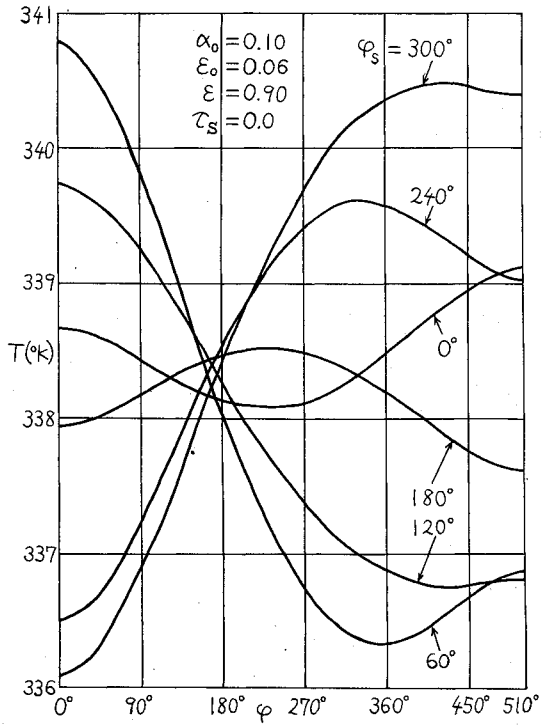

Fig. 2 Circumferential temperature distributions of boom.

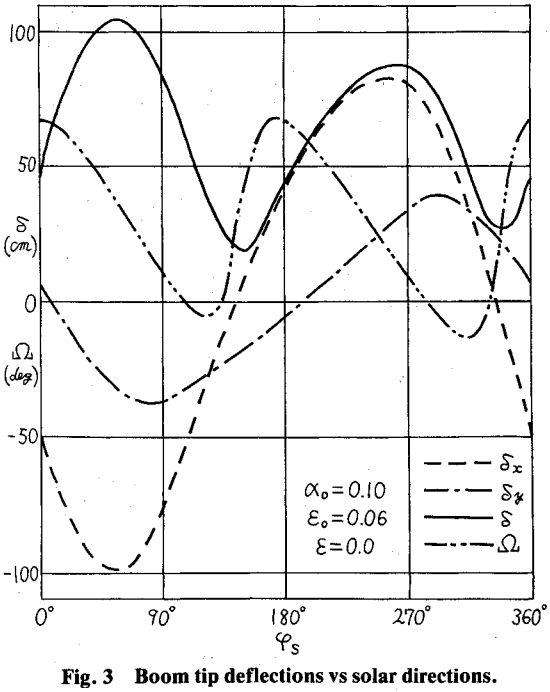

Fig. 3 Boom tip deflections vs solar directions.

From an engineering viewpoint, it is of interest to evaluate the effect of inner surface properties on the solar deflection. Table 3 gives the amount and direction of boom tip deflections estimated for three types of diffuse coatings applied to the inner surface. In Table 3, the symbol δ is defined as $\sqrt{\delta_x^2 + \delta_y^2}$. The results classified as $\epsilon = 0.0$ in the table provide a basis of comparison because they represent the case of no internal radiation exchange. From Table 3, it is seen that the inner surface emittance has an influence on the boom tip deflection to some extent, and that the larger emittance value does not always make the deflection smaller. The results are now discussed from a different standpoint. The tip deflection of a boom of seamless fabrication with an emittance specified as $\epsilon = 0.0$, 0.20, or 0.90 is estimated at 84.5, 83.0, or 76.8 cm, respectively. But, if the boom meets with an eclipse in orbit, they are re-estimated at 84.7, 83.6, and 79.2 cm, respectively, on conditions that $C = 1.78$ J/g·K, $\rho = 1.85$ g/cm^3, and $\zeta = 0.60$. In either case, they are about 80% of the maximum tip deflections obtained from Table 3. Therefore, the seamless fabrication is preferable for smaller tip deflections.

Figure 2 shows the circumferential temperature distributions corresponding to typical directions of solar incidence. The curves are plots of the results calculated for the boom with a diffusely reflecting inside surface specified as $\epsilon = 0.90$. As might have been expected, there is a close correlation between the peak or bottom temperature and the solar direction. The temperature at any point does not vary greatly from the average temperature estimated at 338.3 K. This small temperature excursion extending over the range from 336 to 341 K shows that linearization based upon Eq. (7) does not introduce significant errors in the analytical results.

Figure 3 displays the amount and direction of the solar deflection. This figure is presented for comparison with the curves given by Eby and Karam.[3] For this reason, no internal radiation exchange is taken into account, that is, the computation has been performed on condition that $\epsilon = 0$. The curve representing the x component of the tip deflection is very similar to that given by them in every solar direction. But, with regard to its y component, the agreement between the two is not as good. In spite of this poor agreement, the curves representing the total tip deflection δ and the out-of-sunline angle Ω are roughly the same as those given by Eby and Karam in tendency. From Fig. 3, it can be shown that the maximum tip deflection is about 105 cm. According to their numerical results, it is estimated at about 102 cm. This demonstrates the validity of the analytical method developed in this paper.

Conclusion

Analytical methods based upon differential absorption factors were developed to evaluate wall temperatures and solar deflection of cylindrical structures in space. These methods differ from the conventional ones in applicability, that is, they are applicable to more general cases for which the internal radiation exchange cannot be neglected. One method is associated with a Laplace transformation into which the effect of an eclipse in orbit is incorporated. This approach made it possible to derive the analytical representations which describe temperature distributions for quasisteady states in a boom of seamless fabrication or in a space telescope of long length. Another approach is the variational method, which was adopted for finding the steady-state circumferential temperature distribution of a boom of locked seams. This method was also employed to estimate the temperature nonuniformity in a space telescope into which isothermalizer heat pipes are mounted. Parametric studies were made to obtain technical knowledge helpful to thermal control of large space telescopes and to prediction of thermal behavior for various types of booms.

Appendix A

$$B(\xi,z)=\frac{\mu}{2}\left[\frac{2f}{1-f^2}\{f\cosh\mu(\xi-z)-\cosh\mu(\xi+z)\}+e^{-\mu|\xi-z|}\right] \tag{A1}$$

$$\mu=\sqrt{\epsilon\nu\kappa} \tag{A2}$$

$$\nu=1+\frac{2}{3}\sum_{n=1}^{\infty}\frac{\rho_S^n}{n+2} \tag{A3}$$

$$\kappa=(1-\rho_S)\nu \tag{A4}$$

$$f=\frac{\kappa-\mu}{\kappa+\mu}e^{-2\mu l} \tag{A5}$$

Appendix B

$$g_{11}=\frac{4\epsilon f}{\mu(1+f)}\sinh^2\mu l-\frac{2\epsilon}{\mu}(\mu l-e^{-\mu l}\sinh\mu l)+2\epsilon l$$

$$g_{12}=\frac{4\epsilon f f_4}{\mu^5(1+f)}\sinh\mu l-\frac{\epsilon}{\mu^5}\left[\frac{7}{15}\mu^5 l^5-12\mu l-e^{-\mu l}\{12\mu l\cosh\mu l+(\mu^4 l^4-8\mu^2 l^2-12\mu l-24)\sinh\mu l\}\right]+\frac{7}{15}\epsilon l^5$$

$$g_{22}=\frac{4\epsilon f f_4^2}{\mu^9(1+f)}-\frac{\epsilon}{\mu^9}\left\{\frac{\mu^5 l^5}{5}\left(\frac{107}{126}\mu^4 l^4-\frac{64}{21}\mu^2 l^2-28\right)-(\mu^4 l^4-8\mu^2 l^2-24\mu l-24)f_4 e^{-\mu l}\right\}+\frac{107}{630}\epsilon l^9+\frac{64}{105}\gamma l^7 \tag{B1}$$

where f_4 is defined as

$$f_4=12\mu l\cosh\mu l+(\mu^4 l^4/2-4\mu^2 l^2-12)\sinh\mu l \tag{B2}$$

$$\begin{aligned}
a_{11}&=\frac{\omega_{11}^2-(p_1+k)\omega_{11}/\beta-\lambda_0\omega_{11}+(p_1+k_0)\lambda_0/\beta}{\omega_{11}(\omega_{12}-\omega_{11})(\omega_{21}-\omega_{11})(\omega_{22}-\omega_{11})}\\
a_{12}&=\frac{\omega_{12}^2-(p_1+k)\omega_{12}/\beta-\lambda_0\omega_{12}+(p_1+k_0)\lambda_0/\beta}{\omega_{12}(\omega_{11}-\omega_{12})(\omega_{21}-\omega_{12})(\omega_{22}-\omega_{12})}\\
a_{21}&=\frac{\omega_{21}^2-(p_1+k)\omega_{21}/\beta-\lambda_0\omega_{21}+(p_1+k_0)\lambda_0/\beta}{\omega_{21}(\omega_{11}-\omega_{21})(\omega_{12}-\omega_{21})(\omega_{22}-\omega_{21})}\\
a_{22}&=\frac{\omega_{22}^2-(p_1+k)\omega_{22}/\beta-\lambda_0\omega_{22}+(p_1+k_0)\lambda_0/\beta}{\omega_{22}(\omega_{11}-\omega_{22})(\omega_{12}-\omega_{22})(\omega_{21}-\omega_{22})}
\end{aligned} \tag{B3}$$

$$\begin{aligned}
b_{11}&=(\lambda_0-\omega_{11})/\omega_{11}(\omega_{12}-\omega_{11})(\omega_{21}-\omega_{11})(\omega_{22}-\omega_{11})\\
b_{12}&=(\lambda_0-\omega_{12})/\omega_{12}(\omega_{11}-\omega_{12})(\omega_{21}-\omega_{12})(\omega_{22}-\omega_{12})\\
b_{21}&=(\lambda_0-\omega_{21})/\omega_{21}(\omega_{11}-\omega_{21})(\omega_{12}-\omega_{21})(\omega_{22}-\omega_{21})\\
b_{22}&=(\lambda_0-\omega_{22})/\omega_{22}(\omega_{11}-\omega_{22})(\omega_{12}-\omega_{22})(\omega_{21}-\omega_{22})
\end{aligned} \tag{B4}$$

$$a_{\max}=\frac{\lambda_0}{\beta}\left(a_{11}\frac{1-e^{-\omega_{11}\zeta}}{1-e^{-\omega_{11}}}+a_{12}\frac{1-e^{-\omega_{12}\zeta}}{1-e^{-\omega_{12}}}+a_{21}\frac{1-e^{-\omega_{21}\zeta}}{1-e^{-\omega_{21}}}+a_{22}\frac{1-e^{-\omega_{22}\zeta}}{1-e^{-\omega_{22}}}\right)$$

$$a_{\min}=\frac{\lambda_0}{\beta}\left(a_{11}\frac{e^{-\omega_{11}(1-\zeta)}-e^{-\omega_{11}}}{1-e^{-\omega_{11}}}+a_{12}\frac{e^{-\omega_{12}(1-\zeta)}-e^{-\omega_{12}}}{1-e^{-\omega_{12}}}+a_{21}\frac{e^{-\omega_{21}(1-\zeta)}-e^{-\omega_{21}}}{1-e^{-\omega_{21}}}+a_{22}\frac{e^{-\omega_{22}(1-\zeta)}-e^{-\omega_{22}}}{1-e^{-\omega_{22}}}\right) \tag{B5}$$

$$b_{\max}=\frac{\lambda_0 p_2}{\beta^2}\left(b_{11}\frac{1-e^{-\omega_{11}\zeta}}{1-e^{-\omega_{11}}}+b_{12}\frac{1-e^{-\omega_{12}\zeta}}{1-e^{-\omega_{12}}}+b_{21}\frac{1-e^{-\omega_{21}\zeta}}{1-e^{-\omega_{21}}}+b_{22}\frac{1-e^{-\omega_{22}\zeta}}{1-e^{-\omega_{22}}}\right)$$

$$b_{\min}=\frac{\lambda_0 p_2}{\beta^2}\left(b_{11}\frac{e^{-\omega_{11}(1-\zeta)}-e^{-\omega_{11}}}{1-e^{-\omega_{11}}}+b_{12}\frac{e^{-\omega_{12}(1-\zeta)}-e^{-\omega_{12}}}{1-e^{-\omega_{12}}}+b_{21}\frac{e^{-\omega_{21}(1-\zeta)}-e^{-\omega_{21}}}{1-e^{-\omega_{21}}}+b_{22}\frac{e^{-\omega_{22}(1-\zeta)}-e^{-\omega_{22}}}{1-e^{-\omega_{22}}}\right) \tag{B6}$$

Appendix C

$$B(\psi,\varphi)=(\mu/2)\{\cos\mu(\psi-\varphi)\cot\pi\mu+\sin\mu|\psi-\varphi|\} \tag{C1}$$

$$\mu=\sqrt{\epsilon\nu\kappa/2} \tag{C2}$$

$$\nu=1+2\sum_{n=1}^{\infty}\frac{\rho_S^n}{n+1}\sin\frac{\pi}{n+1} \tag{C3}$$

$$\kappa=(1-\rho_S)\nu \tag{C4}$$

Appendix D

$$f_{11}=2\pi\epsilon_0$$

$$f_{12}=4\pi^4\epsilon_0\left(\frac{\phi'}{3}-\frac{2\pi}{5}\right)+\frac{\epsilon\phi'^5}{30}+\frac{\epsilon\phi^4}{4}\left(\frac{\phi}{5}-\frac{\phi'}{3}\right)-\frac{\epsilon}{2}\left(\frac{\phi'^5}{15}+\frac{\phi^5}{60}-\frac{\phi^4\phi'}{12}-\frac{\pi\phi^4}{6}\right)$$

$$f_{13}=\frac{4\pi^3}{3}\epsilon_0(\phi'-\pi)+\frac{\epsilon\phi'^4}{12}-\frac{\epsilon\phi^3}{6}\left(\phi'-\frac{\phi}{2}\right)-\frac{\epsilon}{2}\left(\frac{\phi'^4}{6}-\frac{\phi^3\phi'}{6}-\frac{\pi\phi^3}{3}\right)$$

$$f_{22}=f'_{22}-\frac{\epsilon f''_{22}}{\mu^4}-\frac{2\epsilon}{\mu^8}(2\phi'k_3-k_1k_2)-\frac{\epsilon}{2\mu^9}\cot\pi\mu\{4\mu^2(2\phi'-k_2)^2+(k_1-k_3)^2\}$$

$$f_{23}=\frac{f'_{23}}{2}+\frac{\epsilon f''_{23}}{2\mu^4}-\frac{\epsilon}{\mu^8}(2\phi'l_3+k_3-k_1l_2-k_2l_1)-\frac{\epsilon}{2\mu^9}\cot\pi\mu\{4\mu^2(2\phi'-k_2)(1-l_2)+(k_1-k_3)(l_1-l_3)\}$$

$$f_{33}=f'_{33}-\frac{\epsilon f''_{33}}{\mu^2}-\frac{2\epsilon}{\mu^8}(l_3-l_1l_2)-\frac{\epsilon}{2\mu^9}\cot\pi\mu\{4\mu^2(1-l_2)^2+(l_1-l_3)^2\} \tag{D1}$$

The definitions of f_{22}, f_{23}, and f_{33} are completed with Eqs. (D2-D5):

$$f'_{22}=32\epsilon_0\pi^7\left(\frac{4\phi'^2}{63}-\frac{\pi\phi'}{6}+\frac{\pi^2}{9}\right)+\frac{\epsilon\phi'^9}{504}-\epsilon\phi^7\left(\frac{\phi'^2}{63}-\frac{\phi'\phi}{48}+\frac{\phi^2}{144}\right)+\frac{\gamma\phi'^7}{105}$$

$$f'_{23}=32\epsilon_0\pi^6\left(\frac{\phi'^2}{9}-\frac{17\pi\phi'}{63}+\frac{\pi^2}{6}\right)+\frac{\epsilon\phi'^8}{112}-\epsilon\phi^6\left(\frac{\phi'^2}{18}-\frac{17\phi'\phi}{252}+\frac{\phi^2}{48}\right)+\frac{\gamma\phi'^6}{30}$$

$$f'_{33}=32\epsilon_0\pi^5\left(\frac{\phi'^2}{20}-\frac{\pi\phi'}{9}+\frac{4\pi^2}{63}\right)+\frac{13\epsilon\phi'^7}{1260}-\epsilon\phi^5\left(\frac{\phi'^2}{20}-\frac{\phi'\phi}{18}+\frac{\phi^2}{63}\right)+\frac{\gamma\phi'^5}{30} \tag{D2}$$

$$f''_{22}=\phi'^5\left(-\frac{1}{5}+\frac{\mu^2\phi'^2}{105}+\frac{\mu^4\phi'^4}{504}\right)+\phi^4\left\{\frac{\phi'}{2}-\frac{3\phi}{10}+\mu^2\phi\left(\frac{2\phi'^2}{15}-\frac{\phi'\phi}{4}+\frac{3\phi^2}{28}\right)-\mu^4\phi^3\left(\frac{\phi'^2}{63}-\frac{\phi'\phi}{48}+\frac{\phi^2}{144}\right)\right\}$$

$$f''_{23}=\phi'^4\left(\frac{1}{2}-\frac{\mu^2\phi'^2}{30}-\frac{\mu^4\phi'^4}{112}\right)-\phi^3\left\{\phi'-\frac{\phi}{2}+\mu^2\phi\left(\frac{\phi'^2}{3}-\frac{37\phi'\phi}{60}+\frac{\phi^2}{4}\right)-\mu^4\phi^3\left(\frac{\phi'^2}{18}-\frac{17\phi'\phi}{252}+\frac{\phi^2}{48}\right)\right\}$$

$$f''_{33}=\phi'^5\left(\frac{1}{30}+\frac{13\mu^2\phi'^2}{1260}\right)+\phi^3\left\{\frac{\phi'^2}{6}-\frac{\phi'\phi}{3}+\frac{2\phi^2}{15}-\mu^2\phi^2\left(\frac{\phi'^2}{20}-\frac{\phi'\phi}{18}+\frac{\phi^2}{63}\right)\right\} \tag{D3}$$

$$k_1=\mu^4\phi'^4/12+\mu^2\phi'^2-6$$

$$k_2=\pi\mu^2\phi^2+2\phi-2\pi$$

$$k_3=\frac{\mu^4\phi^4}{12}+\frac{2\pi\mu^4\phi^3}{3}+\mu^2\phi^2-4\pi\mu^2\phi-6 \tag{D4}$$

$$l_1=\mu^2\phi'(\mu^2\phi'^2/6+1)$$

$$l_2=\pi\mu^2\phi+1$$

$$l_3=\mu^2(\mu^2\phi^3/6+\pi\mu^2\phi^2+\phi-2\pi) \tag{D5}$$

$$K_2=\begin{cases}K_{21} & \text{if} \quad \pi/2\le\varphi_s\le3\pi/2\\ K_{21}+4\pi K_{22} & \text{if} \quad 0\le\varphi_s<\pi/2 \quad \text{or} \quad 3\pi/2<\varphi_s\le2\pi\end{cases}$$

$$K_3=\begin{cases}K_{31} & \text{if} \quad \pi/2\le\varphi_s\le3\pi/2\\ K_{31}+4\pi K_{32} & \text{if} \quad 0\le\varphi_s<\pi/2 \quad \text{or} \quad 3\pi/2<\varphi_s\le2\pi\end{cases} \tag{D6}$$

where K_{21}, K_{31}, K_{22}, and K_{32} are defined as

$$K_{21}=\phi'\left\{\frac{2\varphi_s'^3}{3}+\left(\frac{\pi^2}{2}-4\right)\varphi_s'\right\}$$
$$-\left\{\frac{\varphi_s'^4}{2}+\frac{3}{4}(\pi^2-8)\varphi_s'^2+\frac{\pi^4}{32}-\frac{3\pi^2}{2}+12\right\}$$

$$K_{31}=\phi'\left(\varphi_s'^2+\frac{\pi^2}{4}-2\right)-\left\{\frac{2\varphi_s'^3}{3}+\left(\frac{\pi^2}{2}-4\right)\varphi_s'\right\}$$

$$K_{22}=(\pi\phi'-2\pi^2+3)\cos\varphi_s+\left\{\phi'\left(1-\frac{2\pi^2}{3}\right)+\pi^3-3\pi\right\}\sin\varphi_s$$

$$K_{32}=\left(\frac{\phi'}{2}-\pi\right)\cos\varphi_s-\left(\frac{\pi\phi'}{2}+1-\frac{2\pi^2}{3}\right)\sin\varphi_s \qquad \text{(D7)}$$

The symbol φ_s' in the first two equations of (D7) is connected with φ_s in the following fashion:

$$\varphi_s'=\begin{cases}\varphi_s & \text{if} \quad \pi/2\le\varphi_s\le 3\pi/2\\ \varphi_s+\pi & \text{if} \quad 0\le\varphi_s<\pi/2\\ \varphi_s-\pi & \text{if} \quad 3\pi/2<\varphi_s\le 2\pi\end{cases} \qquad \text{(D8)}$$

References

[1] Frisch, H.P., "Thermal Bending Plus Twist of a Thin-Walled Cylinder of Open Section with Application to Gravity Gradient Booms," NASA TN D-4069, Aug. 1967.

[2] Florio, F.A. and Hobbs, R.B., Jr., "An Analytical Representation of Temperature Distributions in Gravity Gradient Rods," *AIAA Journal*, Vol. 6, Jan. 1968, pp. 99-102.

[3] Eby, R.J. and Karam, R.D., "Solar Deflection of Thin-Walled Cylindrical Extendible Structures," *Journal of Spacecraft and Rockets*, Vol. 7, May 1970, pp. 577-581.

[4] Fixler, S.Z., "Effects of Solar Environment and Aerodynamic Drag on Structural Booms in Space," *Journal of Spacecraft and Rockets*, Vol. 4, March 1967, pp. 315-321.

[5] Graham, J.D., "Radiation Heat Transfer around the Interior of a Long Cylinder," *Journal of Spacecraft and Rockets*, Vol. 7, March 1970, pp. 372-374.

[6] Cummings, R.D., "Thermal Control of the Large Space Telescope (LST)," AIAA Paper 73-720, July 1973.

[7] Katzoff, S., "Studies Relating to Temperature Control of a Large Space Telescope," NASA TN D-7174, May 1973.

[8] Katzoff, S., "Heat Pipes and Vapor Chambers for Thermal Control of Spacecraft," AIAA Paper 67-310, April 1967.

[9] Gebhart, B., "Unified Treatment for Thermal Radiation Transfer Processes—Gray, Diffuse Radiators and Absorbers," ASME Paper 57-A-34, Dec. 1957.

[10] Furukawa, M., "Differential Absorption Factors between Two Area Elements in a Cylinder," *Journal of Spacecraft and Rockets*, Vol. 17, July-Aug. 1980, pp. 378-381.